

# DSC MRI on Rat Model: Choosing the Integration Interval for Measuring CBV

Y-L. Wu<sup>1</sup>, C-C. Chen<sup>1</sup>, Y-C. Wu<sup>1</sup>, C-H. Chang<sup>1</sup>, and F-N. Wang<sup>1</sup>

<sup>1</sup>Biomedical Engineering and Environmental Sciences, National Tsing Hua University, Hsinchu, Taiwan

## Introduction:

The utilization of the Dynamic Susceptibility Contrast (DSC) method to achieve the MR perfusion image is widespread. Conventionally, the cerebral blood volume map is obtained from the curved-fitting of the first pass of the local tissue concentration time curve  $C_T(t)$ , in spite of the fact that it retains some problems such as imperfect fitting or the comparable fast bio-mechanism in small animals that results in few points on the first pass curve for quantification. In this work, we take a closer look at the different integrated parts of  $C_T$ , such as the anterior and posterior part of  $C_T$  peak, direct summation of first pass part, the fitted gamma-variate curve (conventional CBV map), recirculation part, and finally the whole curve. Aiming to observe the characteristics of them, and the results are further compared with the rCBV maps by administration of monocrystalline iron oxide nanoparticles (MION), which features high susceptibility effect and long plasma half-life, were also generated as proportional references for relative quantifications.

## Materials and Method:

According to the principles of DSC perfusion imaging, the area under the first pass curve of the Gd-DTPA  $C_T$  function is proportional to the CBV times the integral of arterial input function. [1] After first passing, the contrast agent bolus is dispersed by pulmonary and system circulations before re-circulating to tissue, and  $C_T$  becomes a stable decreasing function with low concentration. This "recirculation" part of  $C_T$  is usually removed when assessing the CBV value. However, by assuming the AIF as a gradually decreasing function, the area of recirculation is proposed as an alternative index for relative CBV quantification in this study. For small animal imaging, the recirculation CBV can be calculated from more data points in longer duration than the first pass CBV map, and therefore supposed to be less affected by the noise and insufficient sampling rate of applied MRI sequences.

In this study, five normal male Sprague-Dawley rats (mean weight of  $306.98 \pm 29.28$ g) were anesthetized with 1.5% Isoflurane and scanned by a 4.7T animal MRI scanner (Bruker Biospec 47/40). For DSC imaging, 150 consecutive multi-slice gradient echo EPI scans were applied with TE/TR as 25/500 ms, FOV as 32mm, and matrix size as  $64 \times 64$ . 0.3 ml of Gd-DTPA (Magnevist, 469 mg/ mL) was manually injected at the 10<sup>th</sup> second and flushed with 0.5 ml of saline. Relative  $C_T$  was then generated by calculating the  $\Delta R2^*$ . The direct integration of the  $C_T$  curve from contrast agent arriving to the time the value dropping to half maximum was regarded as the direct summation of first pass CBV, while the integration of last 80 data points (i.e. 40 seconds) was utilized for the recirculation CBV. Particularly, the simplified formulation of the gamma variate function [2] was utilized in the fitting to generate the first pass-fitting CBV, by which the maxima value of curve is fixed as well as the time position, to guarantee that those few vital points on the peak are not excised. Moreover, the first pass CBV was constructed by the ascending part CBV and descending part CBV which are separated by the time of the maxima value, to see the characteristics of first pass components. Lastly, the whole curve CBV are generated to be compared as well. (Fig.1) Five pre-MION and Five post-MION gradient echo EPI (TE/TE as 25/2500ms) were then scanned with a Fe dosage of 20mg/kg. The  $\Delta R2^*$  maps by the susceptibility of steady state MION were considered as MION CBV maps and utilized as references for comparison. [3] For comparison of different integrated parts, all relative CBV maps were normalized by its mean value.

## Results :

The normalized standard deviations distributed in each CBV maps are shown in the Fig 2. Note that the high values owned by the conventional first pass-fitting CBVs may result in some sudden bright points in image caused by the ill fitting. Similarly, the significant standard deviations of the descending part CBVs may derive from the fast diluted and dispersed phenomenon of the contrast agent from bolus form, leading to the unstable data distribution, or alternately, may derive from the few data collected at a dramatically decreasing rate, that contributes to the instability. Furthermore, we applied MION CBV maps as references to compare with those six different CBV maps, direct summation of first pass CBVs, ascending part CBVs, descending part CBVs, first pass-fitting CBVs, recirculation CBVs (80 scans), and whole curve CBVs, the  $R^2$  squares were found to be  $0.69 \pm 0.09$ ,  $0.52 \pm 0.11$ ,  $0.45 \pm 0.13$ ,  $0.58 \pm 0.09$ ,  $0.72 \pm 0.11$ ,  $0.76 \pm 0.09$ , respectively. (Fig. 3) Obviously, the weak value of the correlation between the first pass-fitting and MION CBV map casts a doubt on the feasibility. Not surprising that the ascending part and the descending part CBVs reach low values, which the mobility of contrast agent may affect the result. Nevertheless, it's interesting that both lower reliable maps construct the high reliable rCBVs, direct summation of first pass CBVs, which attain the  $R^2$  square value of  $0.6915 \pm 0.09$ . Most importantly, both the recirculation CBVs and the whole curve CBVs possess high correlation values with MION CBV maps conforming to our hypothesis and further revealing its reliability and feasibility.

## Discussion and Conclusion:

According to the results above, the recirculation CBV map holds high relevance to the first pass part. Besides, the superior regressions with MION CBV map insure the advantage of using the recirculation CBV for small animal imaging. The errors of fitting may come from the data recorded by the fast changing peak value, relative low scanning speed of MRI, deviated curve from the empirical gamma-variate model, and even the nonlinearity between  $\Delta R2^*$  and contrast agent concentration around peak value. On the contrary, the recirculation CBV seems more reliable by recruiting more data points for calculation, since the extravasation supposed to be minor in the short duration of DSC imaging. In conclusion, we confirmed the feasibility of using the recirculation part of  $C_T$  for relative CBV measurement. It is also proved that integrating the total area under the  $C_T$  curve including both the first pass and recirculation parts could further enrich the data points and to enhance the reliability.

## Reference

1. Axel L, Radiology 137, 679-86. (1980).
2. Mark T Madsen, Phys. Med. Bid., 1992, Vol. 31, No 1, 1597-1600
3. Mandeville JB et al., MRM 39, 615-24 (1998).

Fig.2 CBV variations of different analyses in rat brain tissue

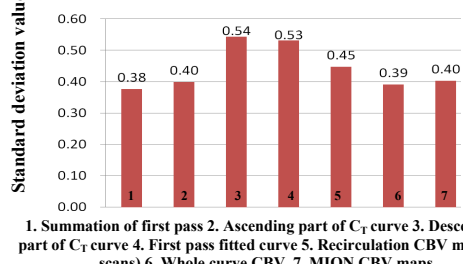


Fig.2: CBV variations of different analyses in rat brain tissue. Both the descending part and the first pass-fitting CBVs possess high standard deviations, which make low resolution images. Both low standard deviations of whole curve CBVs and MION CBVs imply the stable distribution.

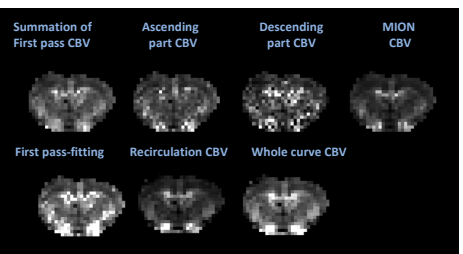


Fig.1: Cerebral Blood Volume maps. Each CBV map is generated from specific integration part of  $C_T$  curve or gamma variate fitting.

Fig.3 R square values between Gd-DTPA and MION injected CBV maps from multiple analyses

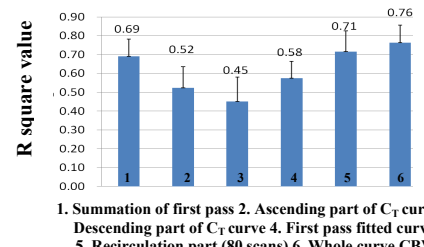


Fig.3: R square values between Gd-DTPA and MION injected CBV maps from multiple analyses. Obviously, the conventional CBV doesn't work well with the correlation between the ideal MION CBVs. And the high correlations of recirculation CBVs and whole curve CBVs suggest their practicalities of utilizing in animal experiments.